Dihydrido and Trihydrido Diolefin Complexes Stabilized by the $Os(PiPr_3)_2$ Unit: New Examples of Quantum Mechanical Exchange Coupling in Trihydrido Osmium Compounds

Amaya Castillo, Miguel A. Esteruelas,* Enrique Oñate, and Natividad Ruiz

Contribution from the Departamento de Química Inorgánica, Instituto de Ciencia de Materiales de Aragón, Universidad de Zaragoza-Consejo Superior de Investigaciones Científicas, 50009 Zaragoza, Spain

Received January 2, 1997[⊗]

Abstract: The hexahydrido complex $OsH_6(PiPr_3)_2$ (**1**) reacts with tetrafluorobenzobarrelene (TFB), 2,5-norbornadiene (NBD), and 1,3-cyclohexadiene to afford $OsH_2(\eta^4\text{-TFB})(PiPr_3)_2$ (**2**), $OsH_2(\eta^4\text{-NBD})(PiPr_3)_2$ (**3**), and $OsH_2(\eta^4\text{-cyclohexadiene})(PiPr_3)_2$ (**4**), respectively. The protonation of **2** and **3** with HBF_4 yields $[OsH_3(\eta^4\text{-TFB})(PiPr_3)_2]BF_4$ (**5**) and $[OsH_3(\eta^4\text{-NBD})(PiPr_3)_2]BF_4$ (**6**). The ^1H NMR spectra of **5** and **6** in the hydrido region at low temperature display AM_2X_2 spin systems ($X = {}^{31}P$), which are simplified to AM_2 spin systems in the $^1H\{^{31}P\}$ spectra. The values for J_{AM} are temperature dependent, increasing from 13.1 to 35.9 Hz (**5**) and from 11.0 to 17.7 Hz (**6**) as temperature is increased from 190 to 230 K and from 180 to 240 K, respectively. The reaction of **4** with HBF_4 leads to the cyclohexenyl complex $[OsH_2(\eta^3\text{-}C_6H_9)(PiPr_3)_2]BF_4$ (**7**), which shows an agostic interaction between the osmium center and one of the two *endo*-CH bonds adjacent to the π-allyl unit. In solution complex **7** is fluxional. The fluxional process involves the exchange between the relative positions of the hydrido ligands and the *endo*-CH hydrogen atoms of the cyclohexenyl ligand and, at the same time, the exchange between the CH allyl and the *exo*-CH hydrogen atoms inside the cyclohexenyl ligand. The structure of **7** in the solid state has been determined by X-ray diffraction. The distribution of ligands around the osmium atom can be described as a piano stool geometry with the agostic hydrogen atom and the midpoints of the carbon−carbon bonds involved in the π-allyl unit forming the three-membered face, while both the hydrido and phosphine ligands lie in the four-membered face.

Introduction

The chemistry of hydrido complexes of transition metals has received increasing attention in recent years,[1] owing to the possibilities offered by these compounds for the design of homogeneous catalysts[2] and the preparation of other types of complexes.[3]

Transition-metal hydrido complexes represent the first example of a quantum mechanical exchange interaction between massive particles at high temperature, and the phenomenon is presently attracting considerable interest. The quantum mechanical exchange coupling is revealed by abnormally large and temperature-dependent hydrogen−hydrogen coupling constants, between the hydrido ligands, which increase with decreasing electron density at the hydride sites. Experimental results show that the magnitudes of the couplings increase in going from neutral to cationic complexes, from third-row to second-row metals and as the π-acceptor character of the coligands is enhanced.[4]

In addition, it is well-known that dienes are good π-acceptor groups, in particular the tetrafluorobenzobarrelene (TFB), 2,5-norbornadiene (NBD), and cyclohexadiene diolefins, as has been previously shown in the chemistry of iridium.[5] So, at first glance, cationic trihydrido diolefin complexes should be good candidates for showing quantum mechanical exchange coupling.

Polyhydrido diolefin complexes have proved to be useful models for understanding catalytic processes related to the hydrogenation of unsaturated organic compounds. However, few such species have been isolated, since they appear to be thermodynamically and kinetically unstable with respect to the other intermediates of the catalytic cycles.[6] In this context, it should be noted that the catalytic mechanisms involve multistep reactions, where the intermediates are connected by equilibria that are highly dependent on the electronic properties and steric requirements of the catalyst ligands, as well as on the characteristics of substrates. Thus, small modifications of these factors can totally change the direction of the equilibria.[2] For a given system, these changes can produce an increase in the activity and selectivity of the system or, on the other hand, the

[⊗] Abstract published in *Advance ACS Abstracts,* September 15, 1997.

(1) (a) Moorl, D.; Robinson, S. D. *Chem. Soc. Rev.* **1983**, *12*, 415. (b) Kubas, G. J. *Acc. Chem. Res.* **1988**, *21*, 129. (c) Jessop, P. G.; Morris, R. H. *Coord. Chem. Rev.* **1992**, *121*, 155. (d) Crabtree, R. H. *Angew. Chem., Int. Ed. Engl.* **1993**, *32*, 789. (e) Heinekey, D. M.; Oldham, W. J. *Chem. Rev.* **1993**, *93*, 913. (f) Gusev, D. G.; Berke, H. *Chem. Ber.* **1996**, *129*, 1143.

(2) Chaloner, P. A., Esteruelas, M. A.; Joó, F.; Oro, L. A. *Homogeneous Hydrogenation*; Kluwer Academic Publishers: Dordrecht, The Netherlands, 1994.

(3) Hlatky G.; Crabtree, R. H. *Coord. Chem. Rev.* **1985**, *65*, 1.

(4) (a) Antiñolo, A.; Chaudret, B.; Commenges, G.; Fajardo, M.; Jalon, F.; Morris, R. H.; Otero, A.; Schweltzer, C. T. *J. Chem. Soc., Chem. Commun.* **1988**, 1210. (b) Jones, D. H.; Labinger, J. A.; Weitekamp, D. P. *J. Am. Chem. Soc.* **1989**, *111*, 3087. (c) Zilm, K. W.; Heinekey, D. M.; Millar, J. M.; Payne, N. G.; Demou, P. *J. Am. Chem. Soc.* **1989**, *111*, 3088. (d) Arliguie, T.; Border, C.; Chaudret, B.; Devillers, J.; Poilbanc, R. *Organometallics* **1989**, *8*, 1308. (e) Heinekey, D. M.; Millar, J. M.; Koetzle, T. F.; Payne, N. G.; Zilm, K. W. *J. Am. Chem. Soc.* **1990**, *112*, 909. (f) Heinekey, D. M.; Payne, N. G.; Sofield, C. D. *Organometallics.* **1990**, *9*, 2643. (g) Arliguie, T.; Chaudret, B.; Jalon, F., Otero, A.; López, J. A.; Lahoz, F. J. *Organometallics* **1991**, *10*, 1888. (h) Heinekey, D. M. *J. Am. Chem. Soc.* **1991**, *113*, 6074. (i) Barthelat, J. C.; Chaudret, B.; Daudey, J. P.; De Loth, Ph.; Poilblanc, R. *J. Am. Chem. Soc.* **1991**, *113*, 9896. (j) Heinekey, D. M.; Harper, T. G. P. *Organometallics* **1991**, *10*, 2891. k) Antiñolo, A.; Carrillo, F.; Fernández-Baeza, J.; Otero, A.; Fajardo, M.; Chaudret, B. *Inorg. Chem.* **1992**, *31*, 5156. (l) Jarid, A.; Moreno, M.; Lledós, A.; Lluch, J. M.; Bertrán, J. *J. Am. Chem. Soc.* **1993**, *115*, 5861. (m) Antiñolo, A.; Carrillo, F.; Chaudret, B.; Fajardo, M.; Fernández-Baeza, J.; Laufranchi, M.; Limbach, H. H.; Maurer, M.; Otero, A.; Pellinghelli, M. A. *Inorg. Chem.* **1994**, *33*, 5163. (n) Gusev, D. G.; Kuhlman, R.; Sini, G.; Eisenstein, O.; Caulton, K. G. *J. Am. Chem. Soc.* **1994**, *116*, 2685.

S0002-7863(97)00021-8 CCC: $14.00 © 1997 American Chemical Society

deactivation of the metallic center. Probably no metallic fragment illustrates this better than the $Os(PiPr_3)_2$ unit, as is reflected by the catalytic properties of the complex $OsHCl(CO)(PiPr_3)_2$[7] and by the number and type of compounds containing carbon donor ligands, which can be isolated with the $Os(PiPr_3)_2$ moiety.[8] Therefore, the $Os(PiPr_3)_2$ unit is an ideal metallic fragment for making an attempt to stabilize trihydrido diolefin complexes.

As a part of our work about the osmium−hydrido chemistry, we have recently reported that the treatment of the hexahydrido complex $OsH_6(PiPr_3)_2$ with 2,2′-biimidazole (H_2biim) leads to the trihydrido compound $OsH_3(Hbiim)(PiPr_3)_2$, which affords the heterobimetallic complexes $(PiPr_3)_2H_3Os(\mu\text{-biim})M(COD)$ by reaction with the dimers $[M(\mu\text{-OMe})(COD)]_2$ (M = Rh, Ir). These biimidazole derivatives show quantum mechanical exchange coupling between the hydrogen nuclei of the OsH_3 unit. The heterobimetallic complexes give rise to larger H−H coupling constants than the mononuclear derivative, and the H−H coupling constants in the heterobimetallic Os−Ir compound are also larger than those found in the Os−Rh derivative.[9]

Continuing with our work in this field, we now report the synthesis of new dihydrido and trihydrido diolefin complexes stabilized by the $Os(PiPr_3)_2$ unit. The trihydrido diolefin complexes are the first derivatives of this type which show quantum mechanical exchange coupling.

Results and Discussion

1. Synthesis and Characterization of OsH_2(diolefin)$(PiPr_3)_2$. Treatment of $OsH_6(PiPr_3)_2$ (**1**) with ca. 5 equiv of tetrafluorobenzobarrelene, 2,5-norbornadiene, and 1,3-cyclohexadiene, in toluene under reflux, gives after 24 h colorless solutions from which the complexes **2**−**4** (Scheme 1) were separated as white solids in good yields (65−78%) by addition of methanol. Two equivalents of diolefin are also hydrogenated to the corresponding monoolefins. Thus, the analysis by gas chromatography of the resulting methanol solutions shows the presence of unreacted diolefin and the corresponding monoolefin in ca. a 1:1 molar ratio.

Scheme 1

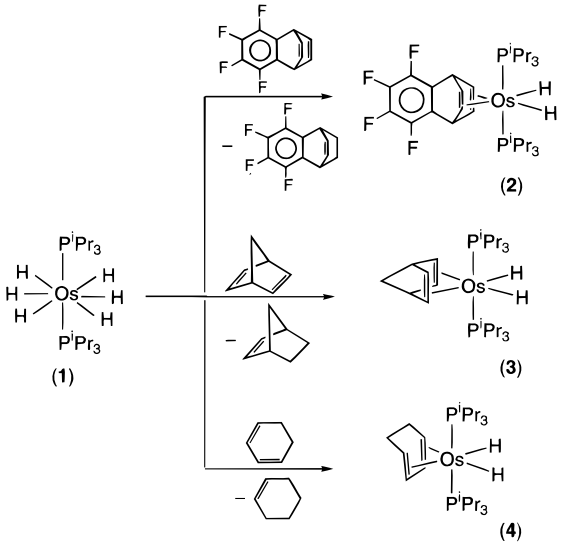

Complexes **2**−**4** were characterized by elemental analysis, IR, and ^{1}H and ^{31}P{^{1}H} NMR spectroscopy. The IR spectra in Nujol show one or two strong absorptions at about 2000 cm^{-1} attributable to the ν(Os−H) vibration, in agreement with a *cis* arrangement of these ligands. The ^{1}H NMR spectra show the hydrido resonances as one triplet between −12.58 and −14.04 ppm, with P−H coupling constants of about 30 Hz, suggesting that both hydrido ligands are chemically equivalent and are *cis* disposed to the phosphine ligands. According to this, the ^{1}H NMR spectrum of **2** contains two diolefinic resonances, one due to aliphatic protons at 5.10 ppm and the other corresponding to the vinylic one at 2.49 ppm. Similarly, the ^{1}H NMR spectrum of **3** contains two aliphatic resonances at 0.98 (−CH_2) and 2.35 (−CH) ppm and one vinylic resonance at 3.71 ppm, and the ^{1}H NMR spectrum of **4** displays two vinylic resonances at 4.64 and 2.76 ppm and one aliphatic at 1.90 ppm. The ^{31}P{^{1}H} NMR spectra of **2** and **3** show singlets at 31.9 (**2**) and 32.2 ppm (**3**), which under off-resonance conditions are split into triplets as a result of the P−H coupling with two hydrido ligands. Although the ^{31}P{^{1}H} NMR spectrum of **4** should display an AB spin system pattern according to the structure proposed for this compound in Scheme 1, only one signal at 28.0 ppm was found at 20 °C and at −40 °C. This signal is also split into a triplet under off-resonance conditions.

We note that the reaction of the tetrahydrido $OsH_4(PEtPh_2)_3$ with 1,5-cyclooctadiene has been previously studied. In contrast to the reactions shown in Scheme 1, treatment of $OsH_4(PEtPh_2)_3$ with 4 equiv of 1,5-cyclooctadiene, in toluene at 100 °C during 65 h, yields $Os(COD)(PEtPh_2)_3$ and cyclooctene.[10]

2. Protonation of 2 and 3. Treatment of complexes **2** and **3** with the stoichiometric amount of HBF_4·OEt_2 in diethyl ether leads to the precipitation of the trihydrido derivatives $[OsH_3(\eta^4\text{-TFB})(PiPr_3)_2]BF_4$ (**5**) and $[OsH_3(\eta^4\text{-NBD})(PiPr_3)_2]BF_4$ (**6**) (eq 1) in high yield (80% (**5**) and 75% (**6**)).

(5) (a) Dragget, P. T.; Green, M.; Lowrie, S. F. W. *J. Organomet. Chem.* **1977**, *135*, C63. (b) Usón, R.; Oro, L. A.; Carmona, D.; Esteruelas M. A. *Inorg. Chim. Acta* **1983**, *73*, 275. (c) Usón, R.; Oro, L. A.; Carmona, D.; Esteruelas, M. A.; Foces-Foces, C.; Cano, F. H.; García-Blanco, S. *J. Organomet. Chem.* **1983**, *254*, 249. (d) Usón, R.; Oro, L. A.; Carmona, D.; Esteruelas, M. A.; Foces-Foces, C.; Cano, F. H.; García-Blanco, S.; Vázquez de Miguel, A. *J. Organomet. Chem.* **1984**, *273*, 111. (e) Usón, R.; Oro, L. A.; Carmona, D.; Esteruelas M. A. *J. Organomet. Chem.* **1984**, *263*, 109. (f) Oro, L. A.; Carmona, D.; Esteruelas, M. A.; Foces-Foces, C.; Cano, F. H. *J. Organomet. Chem.* **1986**, *307*, 83. (g) Fernández, M. J.; Esteruelas, M. A.; Covarrubias, M.; Oro, L. A. *J. Organomet. Chem.* **1986**, *316*, 343. (h) García, M. P.; López, A. M.; Esteruelas, M. A.; Lahoz, F. J. *J. Organomet. Chem.* **1990**, *388*, 365. (i) Esteruelas, M. A.; García, M. P.; López, A. M.; Oro, L. A. *Organometallics* **1991**, *10*, 127. (j) Esteruelas, M. A.; Nürnberg, O.; Oliván, M.; Oro, L. A.; Werner, H. *Organometallics* **1993**, *12*, 3264. (k) Esteruelas, M. A.; Lahoz, F. J.; Oliván, M.; Oñate, E.; Oro, L. A. *Organometallics* **1995**, *14*, 3486.

(6) (a) Baudry, D.; Ephritikhine, M. *J. Chem. Soc., Chem. Commun.* **1980**, 250. (b) Baudry, D.; Ephritikhine, M.; Felkin, H. *J. Organomet. Chem.* **1982**, *224*, 363.

(7) (a) Esteruelas, M. A.; Sola, E.; Oro, L. A.; Meyer, U.; Werner, H. *Angew. Chem., Int. Ed. Engl.* **1988**, 27, 1563. (b) Andriollo A.; Esteruelas, M. A.; Meyer, U.; Oro, L. A.; Sánchez-Delgado, R. A.; Sola, E.; Valero, C.; Werner, H. *J. Am. Chem. Soc.* **1989**, *111*, 7431. (c) Esteruelas, M. A.; Valero, C.; Oro, L. A.; Meyer, U.; Werner, H. *Inorg. Chem.* **1991**, *30*, 1159. (d) Esteruelas, M. A.; Oro, L. A.; Valero, C. *Organometallics* **1991**, *10*, 462. (e) Esteruelas, M. A.; Oro, L. A.; Valero, C. *Organometallics* **1992**, *11*, 3362.

(8) (a) Werner, H.; Esteruelas, M. A.; Otto, H. *Organometallics* **1986**, *5*, 2295. (b) Espuelas, J.; Esteruelas, M. A.; Lahoz, F. J.; Oro, L. A.; Ruiz, N. *J. Am. Chem. Soc.* **1993**, *115*, 4683. (c) Esteruelas, M. A.; Lahoz, F. J.; Oñate, E.; Oro, L. A.; Zeier, B. *Organometallics* **1994**, *13*, 1662. (d) Esteruelas, M. A.; Lahoz, F. J.; López, A. M.; Oñate, E.; Oro, L. A. *Organometallics* **1994**, *13*, 1669. (e) Esteruelas, M. A.; Oro, L. A.; Ruiz, N. *Organometallics* **1994**, *13*, 1507. (f) Esteruelas, M. A.; Lahoz, F. J.; Oñate, E.; Oro, L. A.; Valero, C.; Zeier, B. *J. Am. Chem. Soc.* **1995**, *117*, 7935. (g) Esteruelas, M. A.; Lahoz, F. J.; López, A. M.; Oñate, E.; Oro, L. A. *Organometallics* **1995**, *14*, 2496. (h) Esteruelas, M. A.; Oro, L. A.; Valero, C. *Organometallics* **1995**, *14*, 3596. (i) Bohanna, C.; Esteruelas, M. A.; Lahoz, F. J.; Oñate, E.; Oro, L. A.; Sola, E. *Organometallics* **1995**, *14*, 4825. (j) Esteruelas, M. A.; Gómez, A. V.; López, A. M.; Oro, L. A. *Organometallics* **1996**, *15*, 878. (k) Esteruelas, M. A.; Lahoz, F. J.; Oñate, E.; Oro, L. A.; Sola, E. *J. Am. Chem. Soc.* **1996**, *118*, 89.

(9) Esteruelas, M. A.; Lahoz, F. J.; López, A. M.; Oñate, E.; Oro, L. A.; Ruiz, N.; Sola, E.; Tolosa, J. I. *Inorg. Chem.* **1996**, *35*, 7811.

(10) Bell, B.; Chatt, J.; Leigh, G. J. *J. Chem. Soc., Dalton Trans.* **1973**, 997.

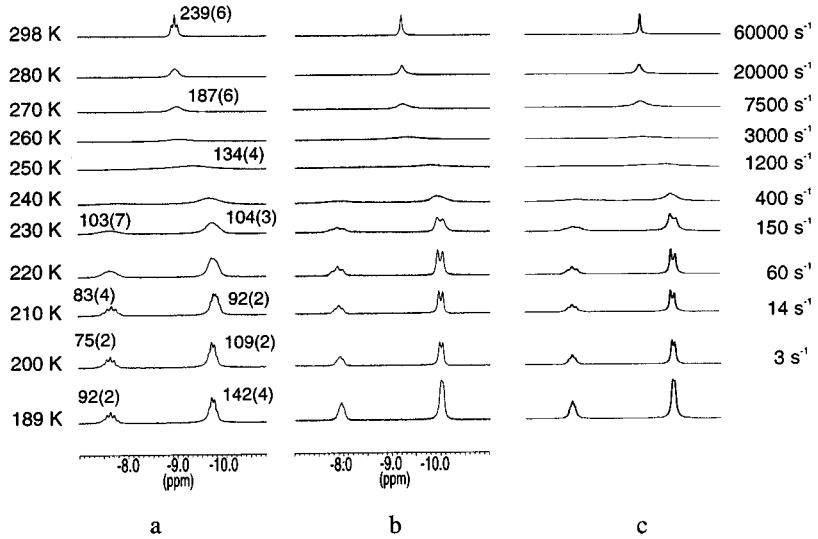

Figure 1. Observed variable-temperature (a) ^{1}H and (b) ^{1}H{^{31}P} NMR spectra (300 MHz) in CD_2Cl_2 in the high-field region of [OsH$_3$(η^4-TFB)(PiPr$_3$)$_2$]BF$_4$ (**5**). (c) Simulated ^{1}H{^{31}P} NMR spectra. T_1, temperatures, and rate constants for the intramolecular hydrogen site-exchange process are also provided.

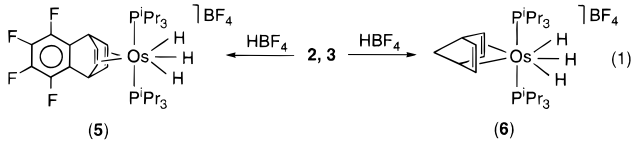

The spectroscopic data of **5** are consistent with the structure proposed in eq 1. The IR spectrum in Nujol shows a ν(Os−H) band at 2164 cm^{-1} along with the absorption due to the [BF$_4$]$^-$ anion with *Td* symmetry, centered at 1090 cm^{-1}. In agreement with the mutually *trans* disposition of the phosphine ligands, at room temperature, the ^{31}P{^{1}H} NMR spectrum in dichloromethane-d_2 shows a singlet at 11.5 ppm, which under off-resonance conditions is split into a quartet due to the P−H coupling with three hydrido ligands. The ^{31}P{^{1}H} NMR spectrum is temperature invariant down to 190 K. However the ^{1}H NMR spectrum is temperature dependent. At room temperature, the spectrum exhibits in the hydrido region a single triplet resonance at −9.15 ppm with a P−H coupling constant of 17.9 Hz. This observation is consistent with the operation of a thermally activated site exchange process, which proceeds at a rate sufficient to lead to a single hydrido resonance. Consistent with this, lowering the sample temperature leads to broadening of the resonance. At very low temperature (240 K), decoalescence occurs and a pattern corresponding to an AM$_2$X$_2$ spin system ($X = {}^{31}$P) is observed, which becomes well resolved at 230 K (Figure 1a). With ^{31}P decoupling (Figure 1b) the spectrum is simplified to the expected AM$_2$ spin system. The values of the chemical shifts of the A ($\delta = -7.8$) and M ($\delta = -10.0$) sites show no significant temperature dependence. However, the magnitudes of the observed H$_A$−H$_M$ coupling constants (J_{AM}) are very sensitive to temperature, increasing from 13.1 to 35.9 Hz as temperature increased from 190 to 230 K (Table 1).

Line shape analysis of the spectra in Figure 1b allows the calculation of the rate constants for the thermal exchange process at different temperatures. The activation parameters obtained from the Eyring analysis are $\Delta H^{\ddagger} = 11.4$ (±0.2) kcal mol^{-1} and $\Delta S^{\ddagger} = 1.6$ (±0.6) cal K^{-1} mol^{-1}. The value for the entropy of activation, close to zero, is in agreement with an intramolecular process, while the value for the enthalpy of activation lies in the range reported for similar thermal exchange processes in other trihydrido− and hydrido−dihydrogen derivatives.[4,9,11]

Table 1. Coupling Constants as a Function of Temperature for **5** and **6**

	J_{obs} (Hz)		J_{ex} (Hz)	
T (K)	**5**	**6**	**5**	**6**
240		17.7		−3.9
230	35.9	16.9	−15.0	−3.5
220	30.1	14.5	−12.1	−2.3
210	23.9	13.3	−9.0	−1.7
200	16.9	12.3	−5.5	−1.2
190	13.1	11.7	−3.6	−0.9
180		11.0		−0.5

To estimate the hydrogen−hydrogen separation between the hydrido ligands, the T_1 values of the hydrogen nuclei of the OsH$_3$ unit were determined over the temperature range 189−298 K.[11a,12] Figure 1a indicates that the T_1 (min) values of the two types of hydridos H$_A$ (73 ms) and H$_M$ (92 ms) do not occur at the same temperature (199 K (H$_A$) and 210 K (H$_M$)), suggesting that the H$_A$/H$_M$ exchange has a significant influence on the observed T_1 times (T_1^{obs}). Between 204 and 189 K, the H$_A$/H$_M$ exchange process is too slow to obtain accurate rate constants (k^{exch}) from the simulation, and they were calculated from $\Delta H^{\ddagger}$ and $\Delta S^{\ddagger}$ (Table 2). In all cases, the obtained values lead to lifetimes τ(H$_A$) and τ(H$_M$), which are much more than the T_1^{obs} time. Under these conditions, we can use eqs 2 and 3, to calculate T_1 values taking into account a slow H$_A$/H$_M$ exchange (T_1^R in Table 2).[13,14]

$$1/T_1^{obs}(H_A) = 1/T_1^{R}(H_A) - {}^2/_3\{T_1^{R}(H_M) + \tau(H_M)\} \quad (2)$$

$$1/T_1^{obs}(H_M) = 1/T_1^{R}(H_M) + {}^1/_3\{T_1^{R}(H_A) + \tau(H_A)\} \quad (3)$$

(11) (a) Earl, K. A.; Jia, G.; Maltby, P. A.; Morris, R. H. *J. Am. Chem. Soc.* **1991**, *113*, 3027. (b) Bautista, M. T.; Cappellani, E. P.; Drouin, S. D.; Morris, R. H.; Schweitzer, C. T.; Sella, A.; Zubkowski, J. *J. Am. Chem. Soc.* **1991**, *113*, 4876. (c) Jia, G.; Drouin, S. D.; Jessop, P. G.; Lough, A. J.; Morris, R. H. *Organometallics* **1993**, *12*, 906.

(12) (a) Crabtree, R. H.; Lavin, M.; Bonneviot, L. *J. Am. Chem. Soc.* **1986**, *108*, 4032. (b) Desrosiers, P. J.; Cai, L.; Lin, Z.; Richards, R.; Halpern, J. *J. Am. Chem. Soc.* **1991**, *113*, 4173. (c) Esteruelas, M. A.; Jean, Y.; Lledós, A.; Oro, L. A.; Ruiz, N.; Volatron, F. *Inorg. Chem.* **1994**, *33*, 3609.

(13) Equations 2 and 3 have been suggested by V. I. Bakhmutov, and they are an expansion of that used for the case of the slow dihydrogen dissociation from IrHX(η^2-H$_2$)(PR$_3$)$_2$.[14]

(14) Bakhmutov, V. I.; Vorontsov, E. V.; Vymenits, A. B. *Inorg. Chem.* **1995**, *34*, 214.

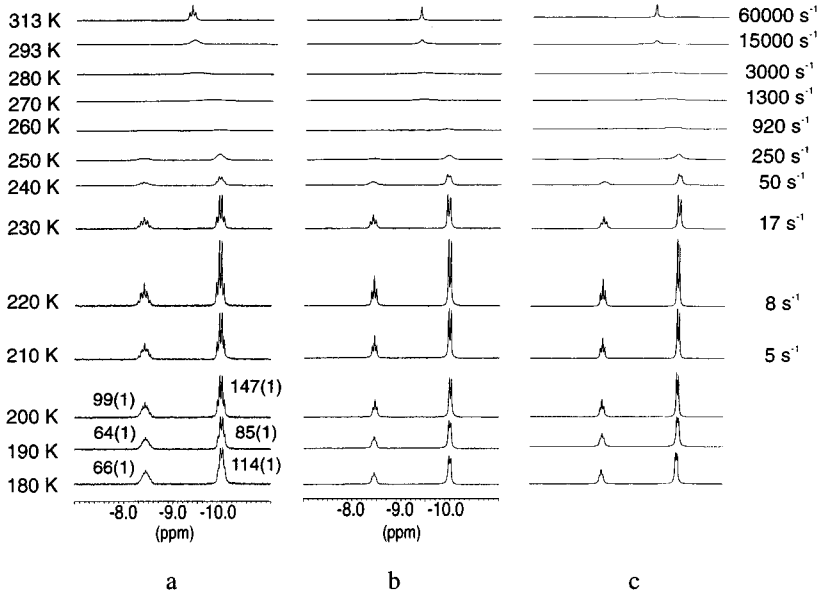

Figure 2. Variable-temperature ^{1}H NMR spectra (300 MHz) in CD_2Cl_2 in the high-field region of $[OsH_3(\eta^4\text{-NBD})(PiPr_3)_2]BF_4$ (**6**). (b) Observed $^1H\{^{31}P\}$ NMR (300 MHz) and (c) simulated spectra. T_1, temperatures, and rate constants for the intramolecular hydrogen site-exchange process are also provided.

Table 2. Variable-Temperature T_1 (ms) Data Observed (T_1^{obs}) and Calculated (T_1^R) Taking into Account the H_A/H_M Exchange for Complex **5** (τ (ms); k^{exch} (s^{-1}))

T (K)	$T_1^{obs}(H_A)$	$T_1^{obs}(H_M)$	k^{exch}	$\tau(H_A)$	$\tau(H_M)$	$T_1^R(H_A)$	$T_1^R(H_M)$
204	80	105	5.987	167	334	71	123
199	73	108	2.885	347	693	**69**	**118**
196	87	125	1.829	547	1094	83	134
189	92	142	0.597	1675	3350	90	146

The T_1^R (min) values calculated in this way are 69 ms for signal A and 118 ms for signal M, and they are obtained at the same temperature, 199 K. From these values, we determine the relaxation rate constant due to hydrido dipole−dipole interactions (R_{HH}), and that due to all other relaxation contributors (R^*), by using eqs 4 and 5,

$$R_A = R^* + 2R_{HH} = 14.5\ s^{-1} \quad (4)$$

$$R_M = R^* + R_{HH} = 8.5\ s^{-1} \quad (5)$$

where $R_A = 1/T_1^R(\text{min})(H_A)$ for the A resonance and $R_M = 1/T_1^R(\text{min})(H_M)$ for the M resonance. Solving for R^* and R_{HH} yields the values 2.5 and 6.0 s^{-1} respectively. From this R_{HH} a hydrido−hydrido separation of 1.7 Å was calculated.[15]

The spectroscopic data of **6** are also consistent with the structure proposed for this complex in eq 1. As for **5**, the most noticeable features of the IR spectrum in Nujol are the ν(Os−H) band at 2147 cm^{-1} and the absorption due to the $[BF_4]^-$ anion with *Td* symmetry centered at 1050 cm^{-1}, which indicates that the anion is not coordinated to the metal center. The $^{31}P\{^1H\}$ NMR spectrum in dichloromethane-d_2 shows a singlet at 12.0 ppm, which is temperature invariant from 240 to 180 K. However, the ^{1}H NMR spectrum (Figure 2), which is similar to that of **5**, is temperature dependent. At room temperature, the spectrum exhibits in the hydrido region a broad resonance centered at −9.40 ppm, which decoalesces into an AM_2X_2 spin system ($X = {}^{31}P$) at 250 K and becomes well resolved at 240 K. In this case, the magnitudes of the observed J_{AM} coupling constants are also temperature dependent, increasing from 11.0 to 17.7 Hz as temperature increased from 180 to 240 K.

(15) $R_{HH} = 129.18/r_{(HH)}{}^6$.

The rate constants for the thermal exchange process at different temperatures were calculated by line shape analyses of the spectra of Figure 2b. The activation parameters obtained from the Eyring analysis are $\Delta H^{\ddagger} = 12.9$ (±0.2) kcal mol^{-1} and $\Delta S^{\ddagger} = 4.5$ (±0.5) cal K^{-1} mol^{-1}.

The T_1 values of the hydrogen nuclei of the OsH_3 unit of **6** were determined over the temperature range 180−200 K. In contrast to those for **5**, the T_1^{obs} (min) values of the H_A (64 ms) and H_M (85 ms) resonances were found at the same temperature (190 K), suggesting that, in this case, there is not a significant influence of H_A/H_M exchange on the T_1^{obs} (min) values. At 190 K, the k^{exch} calculated from $\Delta H^{\ddagger}$ and $\Delta S^{\ddagger}$ is 0.04 s^{-1}, which corresponds to lifetimes $\tau(H_A)$ and $\tau(H_M)$ of 23 and 45 s, respectively. As expected, the T_1^R (min) values obtained by eqs 2 and 3 from these lifetimes are the same as the observed T_1 times. From these values, we determined 1.8 Å as the separation between the hydrido ligands of **6**, by a procedure similar to that previously mentioned for **5**.

The temperature-dependent coupling constant between the hydrido ligands of **5** and **6** can be readily explicable in terms of the exchange coupling between the hydridic protons. From a mechanistic point of view, Limbach, Chaudret, and co-workers have proposed that the exchange coupling involves a metastable dihydrogen complex formed by an activated rate process. Subsequently, rotational tunneling takes place in this dihydrogen.[16]

To rationalize the phenomenon, several theoretical calculations have been also carried out. Lledós and co-workers[17] have studied the quantum mechanical exchange coupling in the trihydrido complexes $Ir(\eta^5\text{-}C_5H_5)H_3L$ (L = PH_3, CO) by combining the construction of ab initio potential energy surfaces with a tunneling model using a basis set method. Although the theoretical exchange coupling values obtained in this way should be taken as an approximation that determines their order of magnitude, the results suggest, in agreement with the dihydrogen proposal, that these transition-metal trihydrido complexes may exchange a pair of hydrogen atoms through a tunneling path, which involves a $M(\eta^2\text{-}H_2)$ transition state.

(16) Limbach, H. H.; Scherer, G.; Maurer, M.; Chaudret, B. *Angew. Chem., Int. Ed. Engl.* **1992**, *31*, 1369.
(17) Jarid, A.; Moreno, M.; Lledós, A.; Lluch, J. M.; Bertrán, J. *J. Am. Chem. Soc.* **1995**, *117*, 1069.

Along this line, Eisenstein and co-workers[18] have calculated the exchange coupling in $OsH_3X(PH_3)_2$ (X = Cl, I) by determining the eigenstates resulting from the coupling between the internal rotation and vibration modes, which correspond to the pairwise hydrogen exchange. The potential has been calculated by core potential ab initio methods. The ratio between the calculated exchange coupling constants for X = Cl and X = I is found to be in good agreement with the experimental ratio though shifted up in temperature.

As an expansion of their previous work,[1e,19] Heinekey and co-workers have recently reported an adaptation of the Landesman results from the work done for the ^{3}He/^{4}He system, which quantitatively models the quantum mechanical exchange coupling observed in certain transition-metal hydrido complexes.[20] In this two-dimensional model, for a given temperature, J_{ex} is determined by three parameters characteristic for each compound which are considered temperature invariant: a, ν, and λ (eqs 6 and 7).

$$J_{ex} = (-\hbar a/2m\pi^2\lambda\delta^2)\exp\{-(a^2+\lambda^2)/2\delta^2\} \quad (6)$$

where

$$\delta^2 = [h/4\pi^2 m\nu\,]\coth[h\nu/2kT] \quad (7)$$

Parameter a is the internuclear distance between the hydrido ligands, ν is believed to describe the H_A-M-H_M vibrational wag mode which allows movement along the H_A-H_M internuclear vector, and λ is the hard sphere radius of the hydrogens. The inclusion of this parameter in the model lowers the probability that the exchange interaction will occur when the hydrogens are too close to each other.

It has generally been accepted that the quantum mechanical exchange coupling is manifest in the ^{1}H NMR spectra of various metal hydrido complexes according to the following expression:[4]

$$J_{AM} = J_{mag} - 2J_{ex} \quad (8)$$

where J_{mag} is the portion of J_{AM} due to the Fermi contact interaction. The sign of J_{mag} is not predicted by eq 8 and may vary from compound to compound. However, according to the proposed model for quantum mechanical exchange coupling, J_{ex} is inherently negative.

By combining eqs 6−8, we obtain eq 9, where, for a given internuclear distance and a given temperature, J_{AM} is determined by J_{mag}, λ, and ν.

$$J_{AM} = J_{mag} + 2[(2\nu\hbar a/\lambda h\coth[h\nu/2kT])\exp\{-2\pi^2 m\nu\,(a^2+\lambda^2)/h\coth[h\nu/2kT]\}] \quad (9)$$

Taking a as the hydrogen−hydrogen separation obtained from the T_1 experiments, we computed the J_{AM} values collected in Table 1 versus the temperature data for **5** and **6**. Plots of the fits are shown in Figure 3. The parameters obtained from the computer fitting are J_{mag} = 6 Hz, λ = 1.1 Å, and ν = 484 cm^{-1} for **5** and J_{mag} = 10 Hz, λ = 1.0 Å, and ν = 496 cm^{-1} for **6** (Table 3). The determined values of J_{mag} were then used to calculate the values of the corresponding J_{ex} at each temperature (Table 1), according to eq 8.

The values of J_{mag} agree well with those previously found in related trihydrido compounds containing the Os(PiPr$_3$)$_2$ unit,[21] whereas similar values of ν and λ have been reported for the complexes $IrH_3(\eta^5\text{-}C_5H_5)(PR_3)$ and $IrH_3(\eta^5\text{-}C_5Me_5)(PR_3)$.[20]

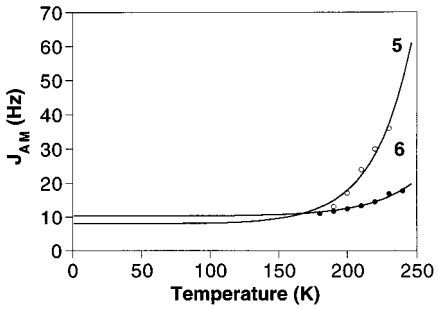

Figure 3. Plots of the fits of the JAM versus temperature date for **5** and **6**.

Table 3. $\Delta H^{\ddagger}$, $\Delta S^{\ddagger}$, a, J_{mag}, λ, and ν for **5** and **6**

complex	$\Delta H^{\ddagger}$ (kcal mol^{-1})	$\Delta S^{\ddagger}$ (cal K^{-1} mol^{-1})	a (Å)	J_{mag} (Hz)	λ (Å)	ν (cm^{-1})
5	11.4 (±0.2)	1.6 (±0.6)	1.7	6	1.1	484
6	12.9 (±0.2)	4.5 (±0.5)	1.8	10	1.0	496

3. Protonation of 4. The cyclohexadiene complex **4** also reacts with HBF_4. Treatment of diethyl ether solutions of **4** with ca. 1 equiv of HBF_4 produces the precipitation of a white solid in 85% yield. According to the elemental analysis, the composition of the solid corresponds to a 1:1 adduct of the fragments $OsH_2(\eta^4\text{-}1,3\text{-cyclohexadiene})(PiPr_3)_2$ and HBF_4.

Although the composition of the solid is similar to those of the complexes **5** and **6**, there are pronounced differences between the $^{31}P\{^1H\}$ and ^{1}H NMR spectra of the white solid and those of **5** and **6**. At room temperature, as for **5** and **6**, the $^{31}P\{^1H\}$ NMR spectrum of the white solid shows a singlet at 34.6 ppm. However, in contrast to the $^{31}P\{^1H\}$ NMR spectra of **5** and **6**, this spectrum is temperature dependent: lowering the sample temperature leads to broadening of the resonance. At 193 K, decoalescence occurs and a pattern corresponding to an AB system is observed, which becomes resolved at 163 K. The ^{1}H NMR spectrum is also temperature dependent. At room temperature the spectrum contains the expected resonances for the triisopropylphosphine ligands along with two broad resonances at 3.55 and −6.90 ppm, with an intensity ratio of approximately 6:5. At 233 K, the resonance at higher field disappears, and from 213 to 173 K, three new resonances are again observed at −8.86, −12.06, and −17.65 ppm (Figure 4). The resonance at 3.55 ppm shows a similar behavior. Lowering the sample temperature leads to broadening of the signal. At 193 K three broad resonances are observed at about 5.7, 5.5, and 3.7 ppm, along with the two broad resonances of the triisopropylphosphine protons at 2.2 and 1.1 ppm which partially hide two signals at about 2.1 and 1.2 ppm. In the IR spectrum in Nujol the most noticeable features are (1) the presence of two ν(Os−H) bands at 2107 and 2182 cm^{-1} and (2) the absorption due to the $[BF_4]^-$ anion with *Td* symmetry centered at 1070 cm^{-1}, which indicates that, in this case, the anion is also not coordinated to the metallic center.

The above-mentioned spectroscopic data suggest that the reaction of **4** with HBF_4 affords the dihydrido cyclohexenyl derivative **7** (eq 10), containing an agostic interaction between the metallic center and one of the two C−H bonds adjacent to the π-allyl unit, which exhibits in solution three proton-exchange processes (Scheme 2).

The *endo*-CH hydrogen atoms adjacent to the π-allyl unit are alternately coordinated to the metal center via a 16-electron

(18) Clot, E.; Leforestier, C.; Eisenstein, O.; Pélissier, M. *J. Am. Chem. Soc*. **1995**, *117*, 1797.

(19) Zilm, K. W.; Heinekey, D. M.; Millar, J. M.; Payne, N. G.; Neshyba, S. P.; Duchamp, J. C.; Szczyrba, J. *J. Am. Chem. Soc*. **1990**, *112*, 920.

(20) Heinekey, D. M.; Hinkle, A. S.; Close, J. D. *J. Am. Chem. Soc*. **1996**, *118*, 5353.

(21) Ruiz, N. Ph.D. Thesis, University of Zaragoza, 1994.

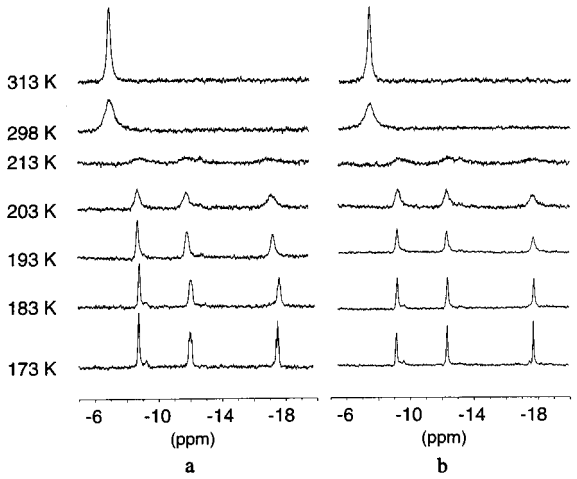

Figure 4. Observed variable-temperature (a) ^1H and (b) $^1H\{^{31}P\}$ NMR spectra (300 MHz) in CD_2Cl_2 in the high-field region of $[OsH_2(\eta^3\text{-}C_6H_9)(PiPr_3)_2]BF_4$ (**7**).

Scheme 2

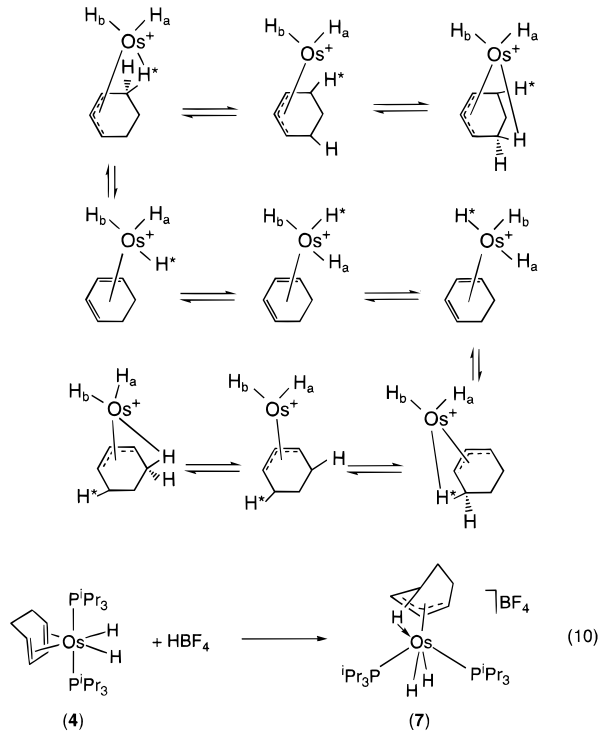

cyclohexenyl dihydrido intermediate. The extraction of the agostic hydrogen atom from the cyclohexenyl ligand by the metal leads to trihydrido diolefin species related to **5** and **6**, which exchange the hydrido position. The migration of one of the three hydrido ligands to either terminal end of the bound diene unit, permitting a degenerate [1,2] metal migration around the ring, produces the exchange of positions between the allyl and *exo*-CH protons.

Operation of the three scrambling modes together results in the separate equilibration of (i) all *endo* hydrogens including the agostic hydrogen and the two hydrido ligands and (ii) all *exo* hydrogens plus the allyl protons. So, the signal at 3.55 ppm in the ^1H NMR spectrum of **7** at room temperature can be assigned to the coalescence between the allyl (3 H) and *exo*-CH (3 H) protons, while that at −6.99 ppm should correspond to the coalescence between the *endo*-CH (3 H) protons and the hydrido ligands (2 H). On the other hand, the spectra of Figure 4 suggest that, in solution at lower temperature than 173 K, complex **7** has the rigid structure shown in eq 10. We assign

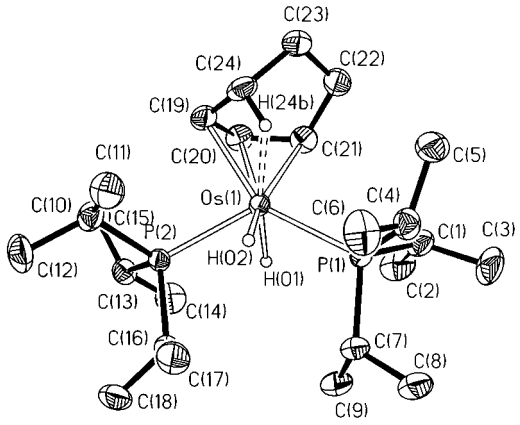

Figure 5. Molecular diagram of the cation $[OsH2(\eta^3\text{-}C_6H_9)(PiPr_3)_2]^+$ (**7**). Thermal ellipsoids are shown at 50% probability.

the resonance at about −9 ppm to the hydrogen atom involved in the agostic interaction, by comparison of the spectra of Figure 4 with that previously reported for the complex $[Ru(\eta^5\text{-}C_5Me_5)\{C_6H_9P(c\text{-}C_6H_{11})_2\}]BF_4$,[22] which contains a cyclohexenyl group coordinated through the carbon−carbon double bond and a strong agostic interaction. Several complexes have also been identified in which a strong agostic interaction is implied by spectroscopic evidence or structurally characterized.[23]

To confirm the agostic interaction within complex **7**, we carried out an X-ray diffraction experiment on a single crystal of this complex. A view of the molecular geometry is shown in Figure 5. Selected bond distances and angles are listed in Table 4, and crystal data are listed in Table 5.

If *M*(1) and *M*(2) are the midpoints of the C(19)−C(20) and C(20)−C(21) bonds, respectively, the distribution of ligands around the osmium atom can be described as a piano stool geometry with the agostic H(24b) hydrogen atom and the midpoints *M*(1) and *M*(2) forming the three-membered face, while both the hydrido and phosphine ligands lie in the four-membered face.

The Os−H(24b) distance of 1.91(6) Å and the Os−C(24) distance of 2.425(6) Å confirm the existence of a strong Os- -H- -C interaction in **7**. These distances, as well as the Os- -H(24b)- -C(24) angle of 109(4)°, are comparable to those found for other agostic interactions in structurally related compounds.[8k,23] The Os- -H(24b)- -C(24) interaction results in some distortion of the cyclohexenyl ligand. The allylic portion of the ring is unsymmetrically bound to osmium; the Os−C(19) distance is shortest at 2.193(5) Å, the Os−C(20) distance is 2.233(5) Å, and the Os−C(21) distance is longest at 2.256(5) Å. Although a similar situation has been found in the complex $Mn\{\eta^3\text{-}C_6H_8(CH_3)\}(CO)_3$,[23c] this differs from the geometry seen in many metal allyl complexes in which the allyl ligand is symmetrically

(22) Arliguie, T.; Chaudret, B.; Jalón, F. A.; Otero, A.; López, J. A.; Lahoz, F. J. *Organometallics* **1991**, *10*, 1888.

(23) See, for example: (a) Howarth, O. W.; McAteer, C. H.; Moore, P.; Morris, G. E. *J. Chem. Soc., Chem. Commun.* **1981**, 506. (b) Lamanna, W.; Brookhart, M. *J. Am. Chem. Soc.* **1981**, *103*, 989. (c) Brookhart, M.; Lamanna, W.; Humphrey, M. B. *J. Am. Chem. Soc.* **1982**, *104*, 2117. (d) Brookhart, M.; Green, M. L. H; Wong, L. L. *Prog. Inorg. Chem.* **1988**, *36*, 1. (e) Selnau, H. E.; Merola, J. S. *J. Am. Chem. Soc.* **1991**, *113*, 4008. (f) Nicholls, J. C.; Spencer, J. L. *Organometallics* **1994**, *13*, 1781. (g) Ogasawara, M.; Saburi, M. *Organometallics* **1994**, *13*, 1911. (h) McLoughlin, M. A.; Flesher, R. J.; Kaska, W. C.; Mayer, H. A. *Organometallics* **1994**, *13*, 3816. (i) Spencer, J. L.; Mhinzi, G. S. *J. Chem. Soc., Dalton Trans.* **1995**, 3819. (j) Carfagna, C.; Deeth, R. J.; Green, M.; Mahon, M. F.; Mclnnes, J.; Pellegrini, S.; Woolhouse, Ch. B. *J. Chem. Soc., Dalton Trans.* **1995**, 3975. (k) Perera, S. D.; Shaw, B. L. *J. Chem. Soc., Dalton Trans.* **1995**, 3861. (l) Galindo, A.; Gutiérrez, E.; Monge, A.; Paneque, M.; Pastor, A.; Pérez, P. J.; Rogers, R. D.; Carmona, E. *J. Chem. Soc., Dalton Trans.* **1995**, 3801.

Table 4. Selected Bond Lengths (Å) and Angles (deg) for the Complex $[OsH_2(\eta^3\text{-}C_6H_9)(PiPr_3)_2]$ BF_4 (**7**)

Bond Lengths			
Os−H(01)	1.57(4)	C(19)−C(24)	1.479(7)
Os−H(02)	1.47(7)	C(20)−C(21)	1.410(7)
Os−P(1)	2.368(1)	C(21)−C(22)	1.521(7)
Os−P(2)	2.339(1)	C(22)−C(23)	1.515(8)
Os−C(19)	2.193(5)	C(23)−C(24)	1.534(7)
Os−C(20)	2.233(5)	C(19)−C(20)	1.422(7)
Os−C(21)	2.256(5)	C(24)−H(24a)	1.02(7)
Os−C(24)	2.425(6)	C(24)−H(24b)	1.00(6)
Os−H(24b)	1.91(6)		
Bond Angles			
P(1)−Os−P(2)	121.78(4)	P(2)−Os−C(20)	101.9(1)
P(1)−Os−C(19)	150.0(1)	P(2)−Os−C(21)	136.9(1)
P(1)−Os−C(20)	129.4(1)	P(2)−Os−H(01)	76(2)
P(1)−Os−C(21)	93.6(1)	P(2)−Os−H(02)	64(3)
P(1)−Os−H(01)	76(2)	P(2)−Os−H(24b)	113(2)
P(1)−Os−H(02)	73(3)	H(01)−Os−H(02)	102(3)
P(1)−Os−H(24b)	99(2)	H(02)−Os−H(24b)	84(3)
P(1)−Os−C(19)	87.3(1)		

Table 5. Crystal Data and Data Collection and Refinement for $[OsH_2(\eta^3\text{-}C_6H_9)(PiPr_3)_2]$ BF_4 (**7**)

Crystal Data	
formula	$C_{24}H_{53}BF_4OsP_2$
mol wt	680.63
color and habit	colorless, irregular prism
cryst size, mm	0.36 × 0.25 × 0.57
symmetry	monoclinic
space group	*P*2/*c* (no. 14)
a, Å	8.868(1)
b, Å	14.115(2)
c, Å	23.388(2)
α, deg	90
β, deg	96.07(1)
γ, deg	90
V, Å^3	2911.1(6)
Z	4
D_{calc}, g cm^{-3}	1.553
Data Collection and Refinement	
diffractometer	four-circle Siemens-Stoe AED
λ (Mo Kα), Å; technique	0.710 73; bisecting geometry
monochromator	graphite oriented
μ, mm^{-1}	4.53
scan type	*ω*/2*θ*
2*θ* range, deg	3 ≤ 2*θ* ≤ 50°
temp, K	213
no. of data collcd	5240
no. of unique data	5106 (R_{int} = 0.0444)
no. of params refined	305
R_1[a] [$F^2 > 2\sigma(F^2)$]	0.0286
wR_2[b] [all data ($F_o \geq 0$)]	0.0842
S[c]	0.980

[a] $R_1(F) = \sum||F_o| - |F_c||/\sum|F_o|$. [b] $wR_2(F^2) = \{\sum[w(F_o^2 - F_c^2)^2]/\sum[w(F_o^2)^2]\}^{1/2}$. [c] GOOF = $S = \{\sum[w(F_o^2 - F_c^2)^2]/(n-p)\}^{1/2}$, where n is the number of observed reflections and p is the number of refined parameters.

bound to the metal with the shortest M−C bond being to the central carbon.[24] In the allylic portion of the ring the C(19)−C(20) and C(20)−C(21) bond lengths of 1.422 (7) and 1.410 (7) are predictably shorter than the aliphatic C−C bonds in the ring which range from 1.515 (8) to 1.534 (7) Å. It is noteworthy that the C(19)−C(24) bond length (1.479 (7) Å) is also significantly shorter than the corresponding C(21)−C(22) distance (1.521 (7) Å) on the opposite side of the ring, suggesting partial multiple-bond character in the C(19)−C(24) bond. A similar feature has been noted in the structure of the manganese complex $Mn\{\eta^3\text{-}C_6H_8(CH_3)\}(CO)_3$.[23c]

(24) Clarke, H. L. *J. Organomet. Chem.* **1974**, *80*, 155.

Concluding Remarks

This study has revealed that the Os(PiPr$_3$)$_2$ unit is an useful fragment in stabilizing polyhydrido diolefin complexes. Thus, the hexahydrido compound $OsH_6(PiPr_3)_2$ reacts with tetrafluorobenzobarrelene, 2,5-norbornadiene, and 1,3-cyclohexadiene to afford the dihydrido diolefin derivatives $OsH_2(\eta^4\text{-TFB})(PiPr_3)_2$ (**2**), $OsH_2(\eta^4\text{-NBD})(PiPr_3)_2$ (**3**), and $OsH_2(\eta^4\text{-cyclohexadiene})(PiPr_3)_2$ (**4**), respectively. The protonation of **2** and **3** leads to the trihydrido diolefin cations $[OsH_3(\eta^4\text{-TFB})(PiPr_3)_2]^+$ (**5**) and $[OsH_3(\eta^4\text{-NBD})(PiPr_3)_2]^+$ (**6**), while under the same conditions, complex **4** yields the dihydrido cyclohexenyl derivative $[OsH_2(\eta^3\text{-}C_6H_9)(PiPr_3)_2]BF_4$ (**7**), which shows an agostic interaction between the osmium center and one of the two *endo*-CH bonds adjacent to the *π*-allyl unit. The trihydrido diolefin cations show quantum mechanical exchange coupling between the hydrogen nuclei of the OsH_3 unit, which fit into the 2D harmonic oscillator model recently reported by Heinekey and co-workers.[20]

In the solid state, complex **7** has a piano stool geometry with the agostic hydrogen atom and the midpoints of the carbon−carbon bonds involved in the *π*-allyl unit forming the three-membered face. In solution, the complex is fluxional. The fluxional process involves the exchange between the relative positions of the hydrido ligands and the *endo*-CH hydrogen atoms of the cyclohexenyl group and, at the same time, the exchange between the allyl and *exo*-CH hydrogen atoms inside the cyclohexenyl ligand.

Experimental Section

All reactions were carried out under an argon atmosphere using standard Schlenk techniques. Solvents were dried using appropriate drying agents and freshly distilled under argon before use. ^{1}H, ^{31}P{^{1}H}, and ^{13}C{^{1}H} NMR spectra were recorded on either a Varian UNITY 300 or on a Bruker 300 AXR spectrometer. The probe temperature of the NMR spectrometers was calibrated at each temperature against a methanol standard. For the T_1 measurements the 180° pulses were calibrated at each temperature. Chemical shifts are expressed in parts per million upfield from Me_4Si (^{1}H and ^{13}C) and 85% H_3PO_4 (^{31}P). Coupling constants (J and N [$N = J(PH) + J(P'H)$ or $J(PC) + J(P'C)$] are given in hertz. IR data were recorded on a Nicolet 550 spectrophotometer. Elemental analyses were carried out with a Perkin-Elmer 240C microanalyzer. The starting complex $OsH_6(PiPr_3)_2$ was prepared by published methods.[25]

Kinetic Analysis. Complete line shape analysis of the spectra ^{1}H{^{31}P} NMR was achieved using the program DNMR6 (QCPE, Indiana University). The rate constants for various temperatures were obtained by visually matching observed and calculated spectra. The transverse relaxation time T_2 used was obtained from spectra for all temperatures recorded, from the line width of the diolefin ligand proton resonances. In complex **7** there is a exchange process involving the hydrido ligands and diolefin protons, so similar values to those obtained for **5** and **6** were used. The activation parameters $\Delta H^{\ddagger}$ and $\Delta S^{\ddagger}$ were calculated by least-squares fit of $\ln(k/T)$ vs $1/T$ (Eyring equation). Error analysis assumed a 10% error in the rate constant and 1 K in the temperature. Errors were computed by published methods.[26]

Preparation of $OsH_2(\eta^4\text{-TFB})(PiPr_3)_2$ (2). A solution of $OsH_6(PiPr_3)_2$ (**1**) (200 mg, 0.39 mmol) in 10 mL of toluene was treated with tetrafluorobenzobarrelene (TFB) (442 mg, 1.95 mmol). The mixture was stirred and heated under reflux for 24 h. The colorless solution obtained was filtered through kieselguhr and concentrated to ca. 0.1 mL. Addition of methanol caused the precipitation of a white solid. The solvent was decanted, and the solid was washed twice with methanol and dried in vacuo. Yield: 285 mg (65%). Anal. Calcd for $C_{30}H_{50}F_4OsP_2$: C, 48.77; H, 6.82. Found: C, 48.77; H, 6.92. IR

(25) Aracama, M.; Esteruelas, M. A.; Lahoz, F. J.; López, J. A.; Meyer, U.; Oro, L. A.; Werner, H. *Inorg. Chem.* **1991**, *30*, 288.

(26) Morse, P. M.; Spencer, M. O.; Wilson, S. R.; Girolami, G. S. *Organometallics* **1994**, *13*, 1646.

(Nujol, cm^{-1}): ν(OsH) 2048, 2036. ^{1}H NMR (300 MHz, C_6D_6, 20 °C): δ 5.10 (br, 2 H, CH(TFB)), 2.49 (br, 4 H, ═CH(TFB)), 2.27 (m, 6 H, PC*H*CH_3), 1.12 (dvt, N = 12.8 Hz, J(HH) = 6.9 Hz, 36 H, PCHC*H*$_3$), −14.04 (t, J(PH) = 30.9 Hz, 2 H, OsH_2). ^{31}P{^{1}H} NMR (121.42 MHz, C_6D_6, 20 °C): δ 31.9 (s; t under off-resonance conditions, $PiPr_3$).

Preparation of $OsH_2(\eta^4$-NBD)$(PiPr_3)_2$ (3). This complex was prepared analogously to that described for **2**, starting from $OsH_6(PiPr_3)_2$ (**1**) (200 mg, 0.39 mmol) and 2,5-norbornadiene (NBD) (212 μL, 1.95 mmol). A white solid was formed. Yield: 163 mg (69%). Anal. Calcd for $C_{25}H_{52}OsP_2$: C, 49.65; H, 8.67. Found: C, 50.01; H, 8.53. IR (Nujol, cm^{-1}): ν(OsH) 2020. ^{1}H NMR (300 MHz, C_6D_6, 20 °C): δ 3.71 (br, 4H, ═CH(NBD)), 2.35 (m, 8 H, PC*H*CH_3 y CH(NBD)), 1.18 (dvt, N = 12.4 Hz, J(HH) = 7.1 Hz, 36 H, PCHC*H*$_3$), 0.98 (br, 2H, CH_2(NBD)), −12.58 (t, J(PH) = 29.7 Hz, 2 H, OsH_2). ^{31}P{^{1}H} NMR (121.42 MHz, C_6D_6, 20 °C): δ 32.2 (s; t under off-resonance conditions, $PiPr_3$). ^{13}C{^{1}H} NMR (75.43 MHz, C_6D_6, 20 °C): δ 62.6 (s, CH_2-(NBD)), 49.0 (s, ═CH(NBD)), 48.5 (s, CH(NBD)), 31.6 (vt, N = 24.9 Hz, P*C*HCH$_3$), 20.0 (s, PCH*C*H$_3$).

Preparation of $OsH_2(\eta^4$-1,3-cyclohexadiene$)(PiPr_3)_2$ (4). This complex was prepared analogously to that described for **2**, starting from $OsH_6(PiPr_3)_2$ (**1**) (200 mg, 0.39 mmol) and 1,3-cyclohexadiene (156 mg, 1.95 mmol). A white solid was formed. Yield: 180 mg (78%). Anal. Calcd for $C_{24}H_{52}OsP_2$: C, 48.63; H, 8.84. Found: C, 48.60; H, 8.40. IR (Nujol, cm^{-1}): ν(OsH) 2044, 1920. ^{1}H NMR (300 MHz, C_6D_6, 20 °C): δ 4.64 (br, 2 H, ═CH), 2.76 (br, 2 H, ═CH), 1.90 (m, 10 H, PC*H*CH_3 y $-CH_2$), 1.16 (dvt, N = 11.8 Hz, J(HH) = 7.3 Hz, 36 H, PCHC*H*$_3$), −12.64 (t, J(PH) = 29.7 Hz, 2 H, OsH_2). ^{31}P{^{1}H} NMR (121.42 MHz, C_6D_6, 20 °C): δ 28.0 (s, t under off-resonance conditions, $PiPr_3$).^{31}P{^{1}H} NMR (121.42 MHz, C_7D_8, −40 °C): δ 28.0 (s, $PiPr_3$). ^{13}C{^{1}H} NMR (75.43 MHz, C_6D_6, 20 °C): δ 65.4 (s, ═CH), 43.9 (t, J(PC) = 7.2 Hz, ═CH), (vt, N = 23.4 Hz, P*C*HCH$_3$), 27.9 (s, CH_2), 20.0 (s, PCH*C*H$_3$).

Preparation of $[OsH_3(\eta^4$-TFB$)(PiPr_3)_2]BF_4$ (5). A solution of $OsH_2(\eta^4$-TFB$)(PiPr_3)_2$ (**2**) (200 mg, 0.27 mmol) in 7 mL of ether was treated with HBF_4 (37 μL, 0.27 mmol). After the mixture was stirred for 5 min at room temperature, a white solid precipitated. The solvent was decanted, and the solid was washed twice with ether and dried in vacuo. Yield: 198 mg (80%). Anal. Calcd for $C_{30}H_{51}BF_8OsP_2$: C, 43.59; H, 6.22. Found: C, 43.21; H, 5.93. IR (Nujol, cm^{-1}): ν(OsH) 2164, $\nu(BF_4)$ 1090. ^{1}H NMR (300 MHz, CD_2Cl_2, 20 °C): δ 5.17 (br, 2 H, CH(TFB)), 3.86 (br, 4 H, ═CH(TFB)), 2.68 (m, 6 H, PC*H*CH_3), 1.38 (dvt, N = 13.7 Hz, J(HH) = 6.9 Hz, 18 H, PCHC*H*$_3$), 1.29 (dvt, N = 14.8 Hz, J(HH) = 7.2 Hz, 18 H, PCHC*H*$_3$), −9.15 (t, J(PH) = 17.9 Hz, 3 H, OsH_3). ^{31}P{^{1}H} NMR (121.42 MHz, CD_2Cl_2, 20 °C): δ 11.5 (s, q under off-resonance conditions, $PiPr_3$).

Preparation of $[OsH_3(\eta^4$-NBD$)(PiPr_3)_2]BF_4$ (6). This complex was prepared analogously to that described for **5**, starting from $OsH_2(\eta^4$-NBD$)(PiPr_3)_2$ (**3**) (200 mg, 0.33 mmol) and HBF_4 (45 μL, 0.33 mmol). A white solid was formed. Yield: 173 mg (75%). Anal. Calcd for $C_{25}H_{53}BF_4OsP_2$: C, 43.35; H, 7.71. Found: C, 43.79; H, 7.30. IR (Nujol, cm^{-1}): ν(OsH) 2147, $\nu(BF_4)$ 1050. ^{1}H NMR (300 MHz, CD_2Cl_2 20 °C) : δ 3.90 (br, 4H, ═CH(NBD)), 2.63 (m, 6 H, PC*H*CH_3), 2.13 (br, 2 H, CH(NBD)), 1.32 (dvt, N = 13.8 Hz, J(HH) = 6.9 Hz, 36 H, PCHC*H*$_3$), 0.97 (br, 2H, CH_2(NBD)), −9.40 (br, 3 H, OsH_3). ^{31}P{^{1}H} NMR (121.42 MHz, CD_2Cl_2, 20 °C): δ 12.0 (s, $PiPr_3$). ^{13}C{^{1}H} NMR (75.43 MHz, CD_2Cl_2, 20 °C) δ 66.3 (s, CH_2(NBD)), 48.1 (s, CH(NBD)), 40.6 (s, ═CH(NBD)), 30.5 (vt, N = 28.1 Hz, P*C*HCH$_3$), 20.1 (s, PCH*C*H$_3$).

Preparation of $[OsH_2(\eta^3$-$C_6H_9)(PiPr_3)_2]BF_4$ (7). This complex was prepared analogously to that described for **5**, starting from $OsH_2(\eta^4$-1,3-cyclohexadiene$)(PiPr_3)_2$ (**4**) (200 mg, 0.29 mmol) and HBF_4 (40 μL, 0.29 mmol). A white solid was formed. Yield: 168 mg (85%). Anal. Calcd for $C_{24}H_{53}BF_4OsP_2$: C, 42.35; H, 7.85. Found: C, 42.62; H, 7.79. IR (Nujol, cm^{-1}): ν(OsH) 2107, 2182, $\nu(BF_4)$ 1070. ^{1}H NMR (300 MHz, CD_2Cl_2, 20 °C): δ 3.55 (br, 6 H, 3 allyl CH and 3 *exo* −CH(C_6H_9)), 2.48 (m, 6 H, PC*H*CH_3), 1.32 (dvt, N = 14.1 Hz, J(HH) = 7.2 Hz, 36 H, PCHC*H*$_3$), −6.90 (br, 5 H, OsH_2 and 3 *endo*-CH-(C_6H_9)). ^{31}P{^{1}H} NMR (121.42 MHz, CD_2Cl_2, 20 °C): δ 34.6 (s, $PiPr_3$). ^{31}P{^{1}H} NMR (121.42 MHz, CD_2Cl_2, −80 °C): δ 33.0 (br, $PiPr_3$). ^{31}P{^{1}H} NMR (121.42 MHz, CD_2Cl_2, −110 °C): δ 28.3, 32.6 (AB system, $J_{PP'}$ = 59.3 Hz). ^{13}C{^{1}H} NMR (75.43 MHz, CD_2Cl_2, 20 °C) δ 47 (br, C_6H_9), 30.1 (vt, N = 26.1 Hz, P*C*HCH$_3$), 19.8 (s, PCH*C*H$_3$).

X-ray Structure Analysis of Complex $[OsH_2(\eta^3$-$C_6H_9)(PiPr_3)_2]$-BF_4 (7). Crystals suitable for an X-ray diffraction experiment were obtained by slow diffusion of ether into a concentrated solution of **7** in CH_2Cl_2. A summary of crystal data and refinement parameters is reported in Table 5. The colorless irregular crystal, of approximate dimensions 0.36 × 0.25 × 0.57 mm, was glued on a glass fibber and mounted on a Siemens-STOE AED-2 diffractometer. Cell constants were obtained from the least-squares fit of the setting angles of 54 reflections in the range $20 \le 2\theta \le 46°$. The 5240 recorded reflections were corrected for Lorentz and polarization effects. Three standard reflections were monitored at periodic intervals throughout data collection: no significant variations were observed. All data were corrected for absorption using a semiempirical (ψ-scan) method.[27] The structure was solved by Patterson (Os atom) and conventional Fourier techniques. Refinement was carried out by full-matrix least-squares with initial isotropic thermal parameters. Anisotropic thermal parameters were used in the last cycles of refinement for all non-hydrogen atoms. Hydrogen atoms, except the hydridos (H(01) and H(02)) and the hydrogens on C(24) (H(24a) and H(24b)), were observed or calculated (C−H = 0.96 Å) and included in the refinement riding on carbon atoms with a common isotropic parameter. The two hydridos, H(24a) and H(24b), were located in the difference Fourier maps and refined as free isotropic atoms. Atomic scattering factors, corrected for anomalous dispersion for Os and P, were implemented by the program.[28] The refinement converged to $R_1 = 0.0286$ [$I > 2\sigma(I)$] and $wR_2 = 0.0842$ (all data, $F^2 > 0$), with weighting parameters $x = 0.0621$ and $y = 5.39$. All calculations were performed by the use of the SHELXTL-PLUS[29] and SHELXL93[28] system of computer programs.

Acknowledgment. We thank the D.G.I.C.Y.T. (Project PB1995-0806, Programa de Promoción General del Conocimiento). We acknowledge Dr. F. Villuendas, Dr. J. Pelayo, and Dr. J. Subias for useful help for computer fitting and Prof. V. I. Bakhmutov for useful discussion about the T_1 determination.

Supporting Information Available: Tables of anisotropic thermal parameters, atomic coordinates and thermal parameters for hydrogen atoms, experimental details of the X-ray study, bond distances and angles, and selected least-squares planes and interatomic distances (24 pages). See any current masthead page for ordering and Internet access instructions.

JA9700212

(27) North, A. C. T.; Phillips, D. C.; Mathews, F. S. *Acta Crystallogr.* **1968**, *A24*, 351.

(28) Sheldrick, G. SHELXL-93. Program for Crystal Structure Refinement, Institüt für Anorganische Chemie der Universität, Göttingen, Germany, 1993.

(29) Sheldrick, G. SHELXTL-PLUS, Siemens Analytical X-ray Inst. Inc., Madison WI, 1990.